

**Syntheses and Structural Determination of New Soluble Transition-Metal Selenides
with Phosphine Ligands**

Presented to the faculty of Lycoming College in partial fulfillment
of the requirements for Departmental Honors in Chemistry

by

Josemar A. Castillo

Lycoming College

April 26th, 2006

Abstract

This project involves the syntheses and characterization of new soluble compounds of the early transition-metal chalcogenides with late transition-metals and phosphine ligands, specifically containing the tetraselenometalate anions $[MSe_4]^{2-}$ ($M=Mo, W$). Our ultimate goal is to grow single-crystals of the compounds, and to determine their structures by single-crystal X-ray diffraction. In this study, new selenide compounds were synthesized by the reaction of $[MSe_4]^{2-}$ with transition-metal chloride salts and triphenylphosphine as the phosphine ligand. These reactions yielded precipitates and in some cases crystal products. Single crystals were sent to the College of William and Mary to be characterized. A new crystal structure described by the formula $[PPh_4]_2[WSe_4] \bullet DMA$ was obtained, however, no new crystalline structures containing $[MSe_4]^{2-}$, a late transition-metal, and a phosphine ligand were characterized. Other crystals are yet to be analyzed.

Introduction

Even though the chemistry of the chalcogens (O, S, Se, and Te) has a long history, most of the compounds that these elements have with transition-metals are insoluble. Chalcogenide complexed with transition-metals are often found as chalcogenide ores.¹ For the past two decades, soluble metal sulfides have been extensively studied because there is evidence of their presence in the active sites of many enzymes, as in the case of nitrogenase, which has an active center containing a Mo/Fe/S complex. This enzyme is able to convert atmospheric nitrogen into ammonia at room temperature, a process that in industry can only be done at extremely high temperature

and high pressure conditions.² Also, a Co/Mo/S surface is present in the catalyst used in the industrial process of hydrodesulfurization (HDS).³ Even though these processes do not involve selenium, selenium complexes can be used as model compounds to understand their chemistry. Researchers also have interest in transition-metal chalcogenide compounds because of their rich structural chemistry.

However, only recently has the chemistry of selenometalates been systematically investigated. In comparison with the analogous thiometalates, only a few compounds containing the anion $[MSe_4]^{2-}$ ($M = Mo, W$) have been fully characterized.⁴ Both tetraselenometalates as well as the tetrathiometalates have been found to be good ligands, especially when combined with a late transition-metals. They show great versatility by retaining their original tetrahedral geometry while allowing other geometries for the late transition-metal. In addition, recent studies in which phosphine ligands were added to tetraselenomolybdate and transition-metals compounds, specifically containing Cu, Ag, or Au, identified the resulting products as having non-linear optical (NLO) properties.⁴

The advantage of studying the chemistry of new soluble transition-metal selenides relies on the idea that they could be used as models to understand the behavior of chalcogens and transition-metal complexes. The presence of selenium, unlike sulfur, allows the application of ^{77}Se NMR to follow the reactions in solution and aid the characterization process. Also the addition of different phosphine ligands to the transition-metal selenides could introduce an interesting structural chemistry to these compounds. Adding to that, the phosphine ligands will most likely increase the solubility of the selenometalate compounds in organic solvents, as well as allowing the use of ^{31}P NMR spectroscopy as another method to follow reaction processes in solution and for

characterization. The coordination numbers and the geometry of the late transition-metal center could vary in unexpected ways.

Literature Review

For the synthesis of new soluble transition-metal selenides it is necessary to start from the soluble tetraselenometalate ions, $[MSe_4]^{2-}$. These anions are analogous to the tetrathiometalate ions $[MS_4]^{2-}$, where M is either tungsten or molybdenum and the anions have a tetrahedral geometry. A convenient method for the synthesis of tetrathiometalate anions involves the use of H_2S in water. However, because of the extreme toxicity of H_2Se , as well as its instability in water (as is $[MSe_4]^{2-}$ in aqueous solution), researchers were able to discover in 1988 a facile method for the synthesis of these tetraselenometalates ions which avoided the use of this undesirable compound.⁵ O’Neal *et al.* were able to prepare $[MSe_4]^{2-}$ in satisfactory yields from the oxidative reaction of polyselenide Se_x^{-2} ($x=2-4$) with the corresponding metal hexacarbonyl, $M(CO)_6$, in dimethylformamide (DMF) solution.⁶



(Ph = C₆H₅)

These anions can then be reacted with organic compounds, selenium and sulfur containing compound, and a variety of transition-metal salts. The formation of mixed-metal selenides is possible after reacting tetraselenometallate anions with transition-metal salts. Tetraphenylphosphonium is a commonly used counter-ion in these kinds of reactions.⁶

Extensive research has already been done in tetrathiometalate and transition-metal complexes. More than two decades ago, several tetrathiometalate and transition-metal complexes were fully characterized, including compounds with phosphine ligands.⁷ The study showed how the tetrathiometalate anions $[MS_4]^{2-}$ with a tetrahedral geometry could coordinate to a late transition-metals (M') with linear (coordination number=2), trigonal planar (coordination number= 3), tetrahedral (coordination number= 4), or octahedral (coordination number= 6) geometry, and how both the metal and the tetrathiometalate anion showed interesting geometry adjustments. Some of these structures are shown in Figure 1. In this figure: the Au in $[Au_2(WSe_3O)_2]^{2-}$ anion has a coordination number of two and is nearly linear; the $[Co(WSe_4)_2]^{2-}$ anion has a tetrahedral Co with coordination number four; the $[Fe(dmso)_2(WS_4)_2]^{2-}$ anion has an octahedral Fe with coordination number six; and the $[Sn_2(WS_4)_4]^{4-}$ anion where both Sn atoms have octahedral geometry. Also, it is worth noticing how the sulfur atoms can be in terminal, μ_2 -bridging, and μ_3 -bridging positions (as seen in the tin complex).

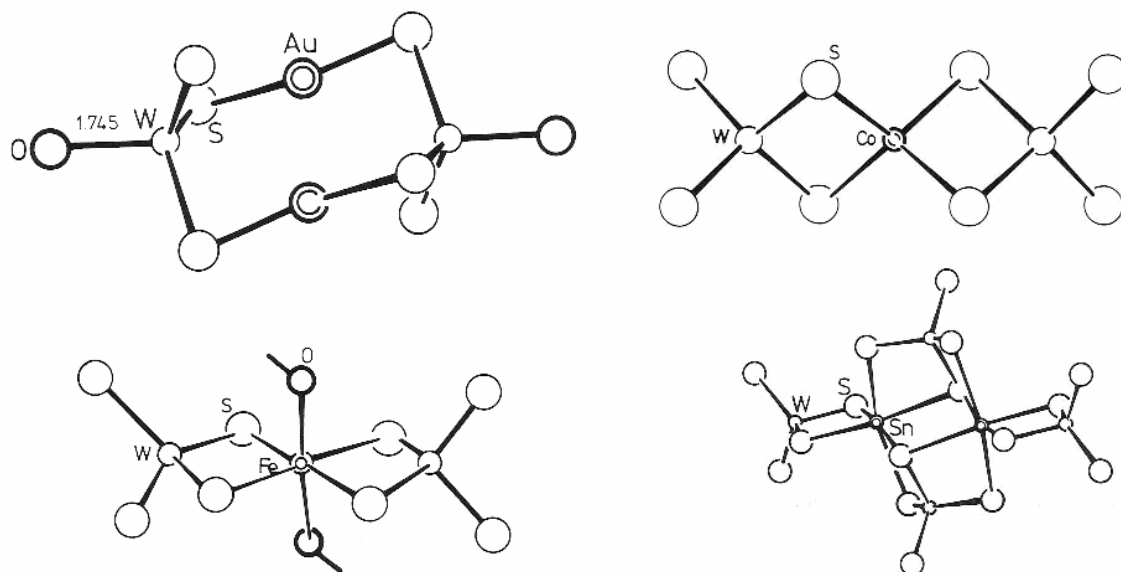


Fig 1. Various coordination geometries of tetrathiometalates and transition-metal complexes.⁷

Following the first preparation of the $[\text{MSe}_4]^{2-}$ by Kolis *et al.*, Ansari and coworkers reported the structure of a $[\text{Ni}(\text{WSe}_4)_2]^{2-}$ anion shown in Figure 2.^{6,8} In 2004, Shiffler and coworkers reported the structure of $[\text{PPh}_4]_2[\text{Pd}(\text{MoSe}_4)_2]$ shown in Figure 3.⁹ Both structures show how the structural chemistry of tetraselenometalate compounds in coordination with transition-metals are analogous to tetrathiometalate compounds first reported by Müller and coworkers (Fig. 1). In both of these tetraselenometalate structures, the late transition-metals Ni^{2+} (Fig. 2) and Pd^{2+} (Fig. 3) have a square planar geometry, while the Se atoms exist in terminal and μ_2 -bridging positions.

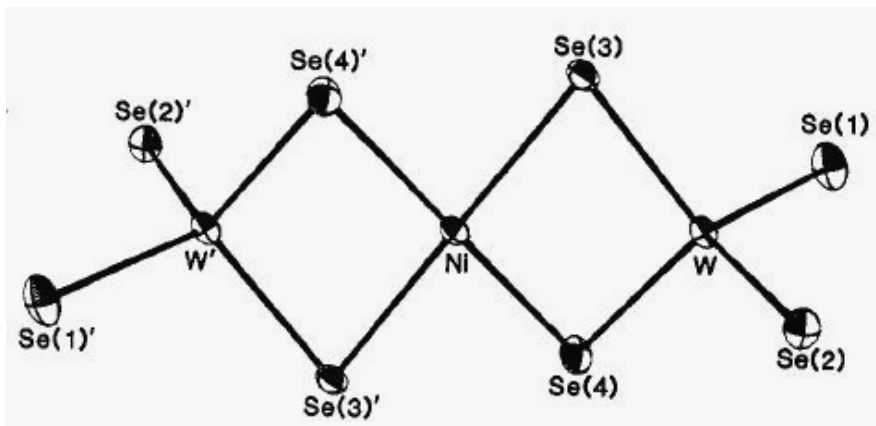


Fig. 2. Structure of $[\text{Ni}(\text{WSe}_4)_2]^{2-}$ synthesized by Ansari *et al.*⁸

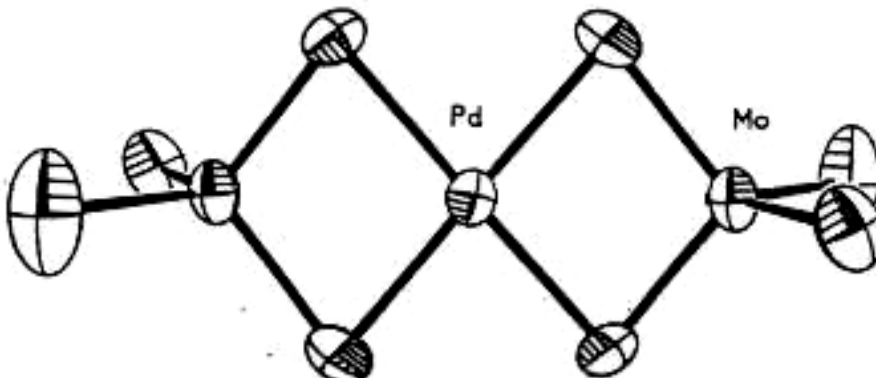


Fig. 3. Structure of $[\text{Pd}(\text{MoSe}_4)_2]^{2-}$ synthesized by Shiffler *et al.*⁹

Müller *et al.* first reported a classic cubane-like cluster compound containing molybdenum, sulfur and phosphine ligands (see Figure 4).⁷ Afterwards, Christuk and coworkers were able to carry the synthesis of metal/[WSe₄]²⁻ cluster compounds with linear, planar and cubane-like geometries at M' where the [WSe₄]²⁻ anion showed great versatility in its coordination to one of the coinage-metal atoms (e.i. Cu, Ag, Au).¹⁰ Some of these compounds are shown in Fig 5-7.

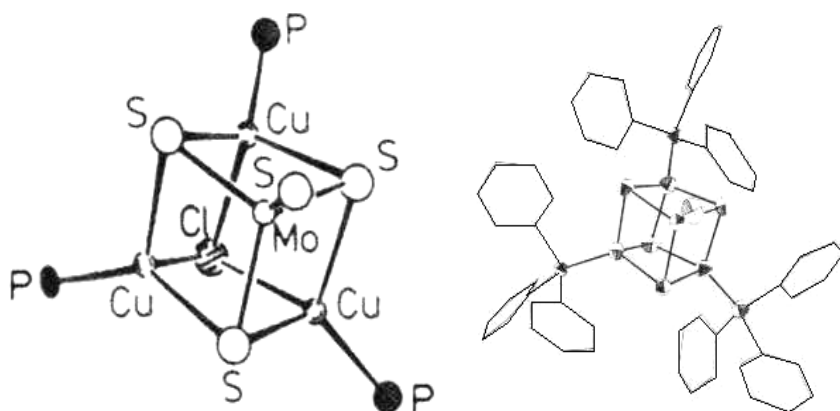


Fig 4. A cubane: $[(\text{Cu}(\text{PPh}_3)_3)(\text{MoS}_4)\text{Cl}]$, the $[\text{MoS}_4]^{2-}$ ligand coordinates all three Cu atoms, which are each tetrahedrally coordinated to two S atoms, one Cl, and one PPh_3 ligand.⁷

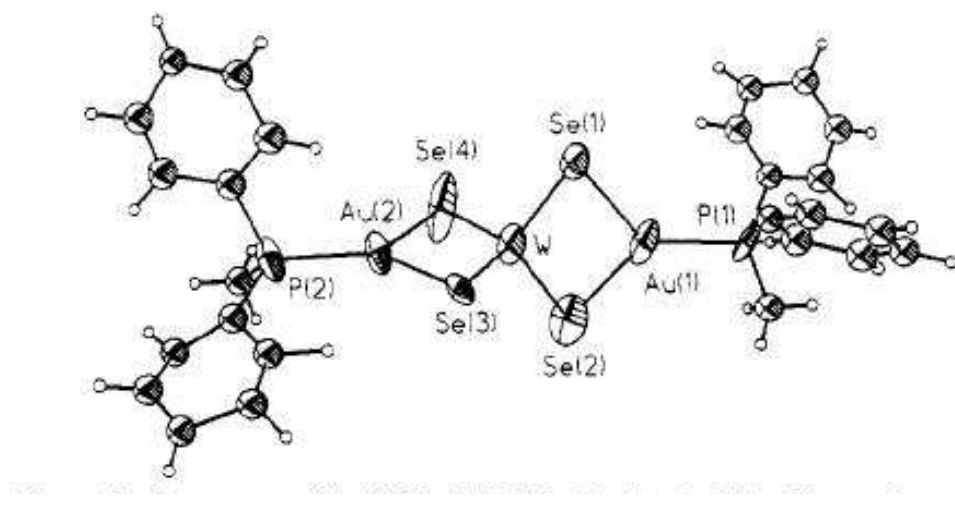


Fig 5. Structure of $(\mu\text{-WSe}_4)[(\text{PMePh}_2)\text{Au}]_2$.¹⁰

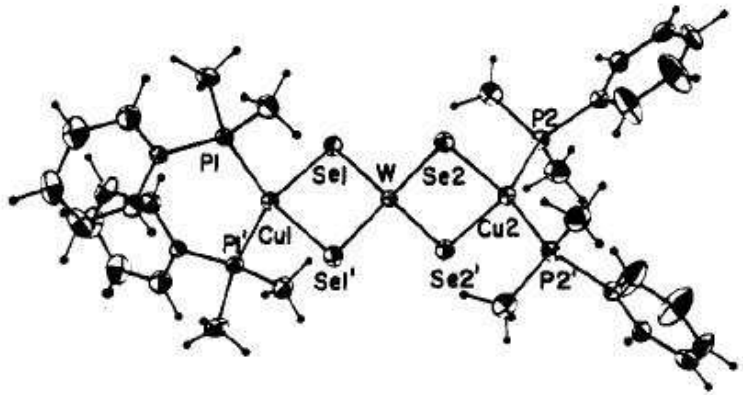


Fig 6. Structure of $(\mu\text{-WSe}_4)[(\text{PMe}_2\text{Ph})\text{Cu}]_2$.¹⁰

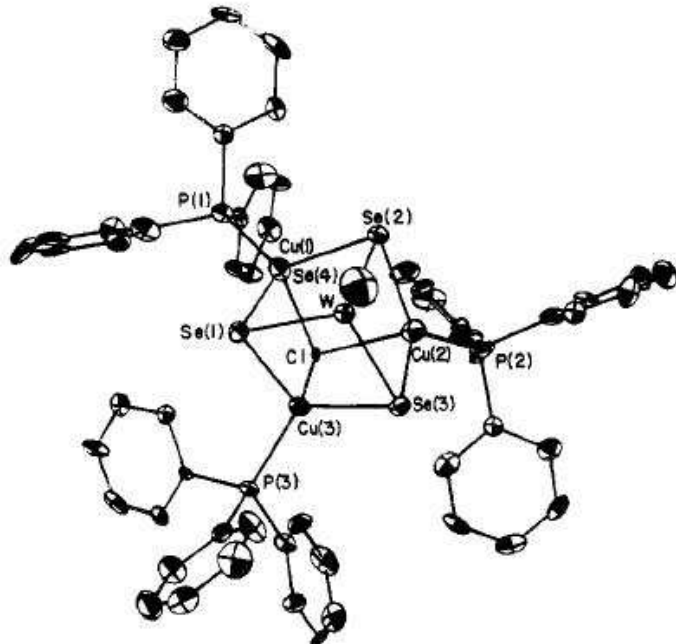


Fig 7. Structure of $(\mu_3\text{-Cl})(\mu_3\text{-WSe}_4)[(\text{PPh}_3)\text{Cu}]_3$.¹⁰

A series of new compounds containing univalent coinage metal atoms and a $[\text{MoSe}_4]^{2-}$ unit were reported by Zhang and coworkers.¹¹ They were able to isolate tetraselenometalate complexes containing either copper, silver or gold and phosphine ligands, which they were able to characterize by ^{95}Mo NMR, IR and Raman

spectroscopies and X-ray crystallography. In this study, they observed how tetraselenometalates can have a variety of geometries and how the late transition-metal can have different coordination numbers; the same behavior previously observed for tetrathiometalate compounds (Fig 1). Figure 8-a shows both M' with coordination number 3; in Figure 8-c both M' have a coordination number of 4; Figure 8-b shows two M' having coordination numbers of 3 and 4. Figure 8-d is a cubane structure where one MQ_4 unit coordinates three late-transition metals. In these compounds Se can be in both μ_2 and μ_3 bridging bonding modes (shown in Fig 8 a-c and Fig 8-d respectively), as well as appear in a terminal position (shown in Fig 8-d).¹¹

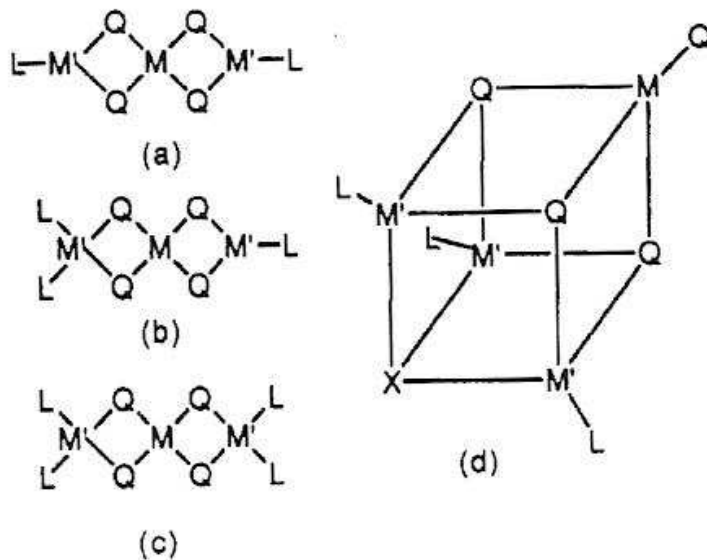


Fig 8. Sketch of known structures containing the MQ_4^{2-} core ($\text{Q}=\text{S, Se}; \text{M}=\text{Mo, W}; \text{M}'=\text{Ag, Au, Cu}; \text{L}=\text{ligand}; \text{X}=\text{Cl or Br}$).¹⁰

$[\text{MoSe}_4(\text{AuPPh}_3)_2]$ is one of the anions that Zhang and coworkers synthesized. Its molecular structure is shown in Figure 9 (this compound shows the specific arrangement in Fig 8-a).¹¹

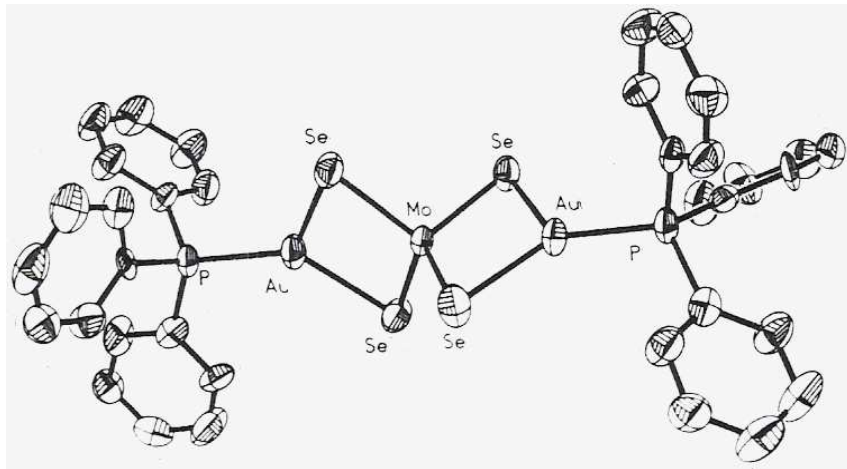


Fig 9. The molecular structure of the compound $[\text{MoSe}_4(\text{AuPPh}_3)_2]$ synthesized by Zhang *et al.*¹¹

In 2002, the structure, reactivity and potential non-linear optical (NLO) properties of coordination cluster compounds of tetraselenomolybdate anions with transition-metals were reviewed by Zhang and coworkers. Their study focused on the synthesis and structure of coordination cluster compounds with tetraselenomolybdate and tetraselenotungstate anions as polydentate ligands. They incorporated phosphine ligands into the selenometalate complexes and evaluated these structures as potential non-linear optical materials.⁴ Zhang *et al.* noticed a strong relationship between the structure of the tetraselenometalate complexes and their NLO properties. They also observed how these compounds show many advantages in comparison to their sulfur analogs, not only in their NLO properties, but also in how heteroselenometallic clusters showed larger optical limiting effects than the analogous sulfur clusters. This difference in behavior concerning NLO properties can be attributed to the heavy atom effect (Se rather than S) and it is dependent on the skeletal atoms of the compounds.¹² The higher limiting threshold of the compounds studied by Zhang and coworkers could also be explained by the electronic effect of the organic ligands (like PPh₃), which at specific geometries tend to move

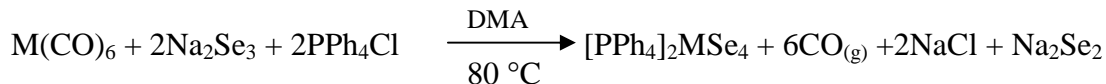
electron density from the late transition-metal fragments towards the $[MSe_4]^{2-}$ moiety, resulting in delocalization of electron density among the metal atoms.⁴

Because of their advantages as model compounds, their rich structural chemistry and their potential as non-linear optical materials, the focus of our particular research is the synthesis of new soluble transition-metal selenides with phosphine ligands. The ultimate goal of this study is to be able to grow single crystals of these compounds in order to determine their structures by single-crystal X-ray diffraction studies. Previously in our lab, reactions were done with tetraselenometalates compounds, a variety of transition-metals, and different phosphine ligands (PPh_3 and dppe). While new compounds were apparently made, and single crystals were sent to Anjou University in South Korea, no new compounds containing the $[MSe_4]^{2-}$ unit complexed with a transition-metal and phosphine ligands were characterized.

Infrared and ultraviolet-visible spectroscopy will also be used for the characterization of intermediate and final products. After characterizing the new compounds, it would be of interest to compare them with the analogous sulfides. Hopefully, in the future, the results of this project would enhance the understanding of chemical and biological processes involving transition-metal chalcogenides.

Results and Discussion

Syntheses and Spectroscopy. Kolis and co-workers first prepared $[MSe_4]^{2-}$ ($M= Mo, W$) in high yields by the convenient reaction of metal carbonyls $M(CO)_6$ with Se_3^{2-} in DMF.⁶ In our study, the tetraselenometalates were obtained as their tetraphenylphosphonium salts with a yield of 49.5% for $[MoSe_4]^{2-}$ and 64.5% for $[WSe_4]^{2-}$ using dimethylacetamide (DMA) as the solvent for the following reaction.



The mechanism for the formation of the selenometalate anions $[MSe_4]^{2-}$ from the metal carbonyls is unknown (and it was previously unexpected). Formally, the reaction involves an oxidation of the metal center from 0 to 6+. Here, Se_3^{2-} is acting as the oxidizing agent. As was previously reported, heating the reaction makes it proceed more quickly; however, the reaction still occurs at room temperature after stirring for several days.⁶ The tetraselenometalate anions were characterized by infrared and UV-vis spectroscopy. For thiometalates anions and sulfide system in general, infrared spectroscopy is a valuable tool for characterization, however, this technique is less valuable for the characterization of selenometalate anions, $[MSe_4]^{2-}$.^{9, 11} The reason being that Mo-Se vibration absorptions usually appear in the fingerprint region of $400-200\text{ cm}^{-1}$ which makes its identification through IR a difficult task, since the available IR spectrometer for our study only goes down to 400 cm^{-1} .⁹

More than two decades ago, Müller and co-workers reported a series of anionic mixed metal sulfides.⁷ In these $[M'(MS_4)_n]^{2-}$ ($M= Mo, W$; $M'= Fe^{2+}, Co^{2+}, Ni^{2+}, Pd^{2+}$,

Pt^{2+} , Zn^{2+} , Cd^{2+} and Hg^{2+} , $n=2$) anions, the $[\text{MS}_4]^{2-}$ unit was found to retain a nearly tetrahedral geometry when bound to a M' center, while allowing the preferred geometry of the late transition-metal. Later studies started investigating the analogous selenium anions.⁴ Similar results were obtained by Ansari and co-workers, who reported the tetraselenotungstate anions bound to Ni^{2+} and Pd^{2+} centers.⁸ The versatility of the tetraselenometalates was also shown by the compounds synthesized by Zhang *et al.* who reported a series of compounds containing a late transition-metal (Cu, Ag and Au), the tetraselenomolybdate unit and phosphine ligands. The phosphine ligands increase the solubility of the final compound in organic solvents, and it was also found that non-linear optical properties were characteristic in the resulting compound.¹¹

In this project, a typical reaction consisted of weighing the three specific reagents, as indicated by the reaction equation shown below, into a Schlenk flask inside of a glove box. The flask was then transferred to a Schlenk line and by using standard Schlenk techniques under an inert atmosphere (N_2 or Ar), DMA or acetonitrile was added by syringe, and the reaction was left stirring at room temperature for a minimum of three hours. The reaction was then layered with tetrahydrofuran (THF) and put in the freezer overnight at approximately -20°C to encourage the formation of crystals. In some cases diethyl ether was also used in the layering process whenever THF alone did not make the products of the reaction fall out of solution.



($\text{M}= \text{W, Mo}; \text{ M}'= \text{Pt}^{2+}, \text{Ru}^{2+}, \text{Eu}^{3+}, \text{Ni}^{2+}, \text{Co}^{2+}, \text{Sm}^{3+}, \text{Tb}^{3+}, \text{Fe}^{2+}, \text{Cr}^{3+}, \text{Zn}^{2+}; n= 2,3$)

When a precipitate was formed as result of the reaction, it was filtered and washed with ether to ensure complete dryness. If crystals were formed, they were examined under a microscope. In the early stages of the study, if the crystals showed enough stability when exposed to a non-inert gas atmosphere, attempts were made to place single crystals into capillaries with the purpose of using X-ray diffraction studies for their characterization. However, it was necessary that crystals of the novel compounds were stable when in brief contact with air, because we did not have the equipment necessary to analyze the crystals under the microscope and place them into capillaries under a N₂ or Ar atmosphere. Because of this, single crystals were difficult to collect and they tended to decompose before they could be characterized. Recently, we were able to purchase a glove bag to solve this problem. Crystal mounting can now be done under an inert atmosphere, and as expected, the collection of single crystals in capillaries is possible, avoiding the decomposition of the final products. The single crystals collected were sent to the College of Williams and Mary in order to be analyzed. No new transition-metal tetraselenometalate complex has been characterized up till now, however, a new crystalline structure with the formula [PPh₄]₂[WSe₄]•DMA has been found. More crystals were sent recently to the College of William and Mary for further X-ray diffraction studies.

In this study, the reaction system yielded novel soluble transition-metal selenide compounds with phosphine ligands (Table. 1).

Table 1. Summary of significant reactions. The phosphine ligand used in all the reactions was triphenyl phosphine, PPh₃. (*)Have been sent for X-ray crystallographic studies.

(PPh ₃) ₂ (MSe ₄) M= Mo or W	M'Cl _n	Solvent	Layering solvent	Result
Mo	Pt ²⁺	DMA	THF, ether	Gray precipitate / Brown crystals
W	Pt ²⁺	DMA	THF, ether	Tan precipitate/ Dark orange crystals
W	Pt ²⁺	CH ₃ CN	THF	No precipitate/crystals
Mo	Ru ³⁺	DMA	THF	No precipitate/crystals
W	Ru ³⁺	DMA	THF, ether	Dark Blue precipitate/ Clear green crystals
W	Ru ³⁺	CH ₃ CN	THF	Dark gray precipitate/ Yellow crystals
W	Ru ³⁺	CH ₃ CN	THF	Dark green precipitate
Mo	Ni ²⁺	DMA	THF	Pale yellow precipitate
W	Ni ²⁺	DMA	THF	Red crystals *
W	Ni ²⁺	CH ₃ CN	THF	Pale precipitate
Mo	Co ²⁺	DMA	THF, ether	Pale turquoise precipitate
Mo	Co ²⁺	CH ₃ CN	THF	Gray precipitate
Mo	Sm ³⁺	DMA	THF	Blue crystals *
W	Sm ³⁺	DMA	THF	Red crystals *
W	Fe ²⁺	DMA	THF	No precipitate/crystals
W	Fe ²⁺	CH ₃ CN	THF	Dark brown precipitate
Mo	Cr ³⁺	DMA	THF	Blue Crystals *
W	Cr ³⁺	DMA	THF	No precipitate/crystals
W	Cr ³⁺	CH ₃ CN	THF	Black precipitate

$(PPh_4)_2(MSe_4)$ M= Mo or W	$M'Cl_n$	Solvent	Layering solvent	Result
W	Eu^{3+}	DMA	THF	Red precipitate
W	Zn^{2+}	DMA	THF	Green crystals *
W	Zn^{2+}	CH_3CN	THF	Dark brown precipitate
Mo	Tb^{3+}	DMA	THF	Blue crystals
W	Tb^{3+}	DMA	THF	Red crystals (small)/ Orange crystals (large)

Precipitates of the reaction products were more likely to be obtained when the reactions were run in acetonitrile (CH_3CN), which is consistent with the fact that this solvent is less polar than DMA and does not dissolve the products as well. However, reactions with DMA as a solvent had more tendency to form crystals, as was the case of the reaction of $[WSe_4]^{2-}$, Ni^{2+} and PPh_3 , which yielded bright red needle-like crystals, and the reaction of $[WSe_4]^{2-}$, Ru^{2+} and PPh_3 , which produced yellow needle crystals. The reactions that yielded crystals are indicated in Table 1 (bold).

In the reactions of both $[WSe_4]^{2-}$ and $[MoSe_4]^{2-}$ with Pt^{2+} , including triphenylphosphine as the phosphine ligand, crystals were produced only if the solution was layered with ether. The use of ether as the layering solvent was also necessary to obtain a precipitate in the reaction of $[MoSe_4]^{2-}$, Co^{2+} , and PPh_3 . In these specific reactions, the products were too soluble to come out of solution if only THF was used in the layering process; the resulting brownish crystals in the reaction with Pt^{2+} grew on the walls of the Schlenk flask, however, they were really fragile and therefore could not be successfully collected. The use of ether in the reaction of $[WSe_4]^{2-}$ with Ru^{3+} also encouraged the formation of crystals. Nevertheless, they were clear green, and because of

this particular appearance it was assumed that the crystals do not represent new compounds worth collecting.

Product precipitate was obtained for all the reactions of $[\text{MSe}_4]^{2-}$ with M' chloride salts ($\text{M}' = \text{Ru}^{3+}, \text{Co}^{2+}, \text{Ni}^{2+}, \text{Pt}^{2+}, \text{Cr}^{3+}, \text{Zn}^{2+}, \text{Fe}^{2+}$ and Eu^{2+}) and PPh_3 , except for the reaction of $[\text{MoSe}_4]^{2-}$ with Ru^{3+} , and $[\text{WSe}_4]^{2-}$ with $\text{Cr}^{3+}, \text{Zn}^{2+}$, and Fe^{2+} (all in DMA and PPh_3 as the phosphine ligand) and $[\text{WSe}_4]^{2-}$ with Pt^{2+} in acetonitrile. Even though crystals were produced in some reactions, not all could be collected and some were not suitable for X-ray crystallographic studies, which is the reason why they have not yet been characterized structurally. Some crystals showed air-sensitivity, while others remained unchanged even when they were outside of the glove box. Examples of these are the apparent crystals yielded in the reaction with Tb^{3+} and both $[\text{WSe}_4]^{2-}$ and $[\text{MoSe}_4]^{2-}$. These crystals were relatively soft which made them really hard to place into capillaries.

The evidence of the successful reactions is based on infrared and, whenever possible, UV-vis spectroscopy. Spectra of starting materials as well as products were taken when possible. The vibration stretches M-Se (terminal), Me-Se (bridging), M-Se (ring), and Se-Se, all appear at similar regions in the infrared spectrum ($200\text{-}340\text{ cm}^{-1}$) as indicated by Ansari and coworkers. Therefore, the characterization of products by this means is not viable due to the fact that we cannot see this part of the IR with our spectrometer. All complexes synthesized here show intense bands in their infrared absorption spectra that can be used for identification purposes. X-ray crystallography studies are necessary to obtain structures of the novel compounds synthesized in this study.

The red crystals that were obtained as the product of the reaction between $[\text{WSe}_4]^{2-}$, Ni^{2+} , and PPh_3 were found to be the starting material, $[\text{PPh}_4]_2[\text{WSe}_4]\bullet\text{DMA}$ after the crystal structure was solved through X-ray diffraction analysis. However, this is a new crystalline structure which is first reported in our present study. Crystallographic details of the $[\text{PPh}_4]_2[\text{WSe}_4]\bullet\text{DMA}$ [1] structure are given in Figure 10, and Tables 2 and 3 (more details can be found in supplementary material).

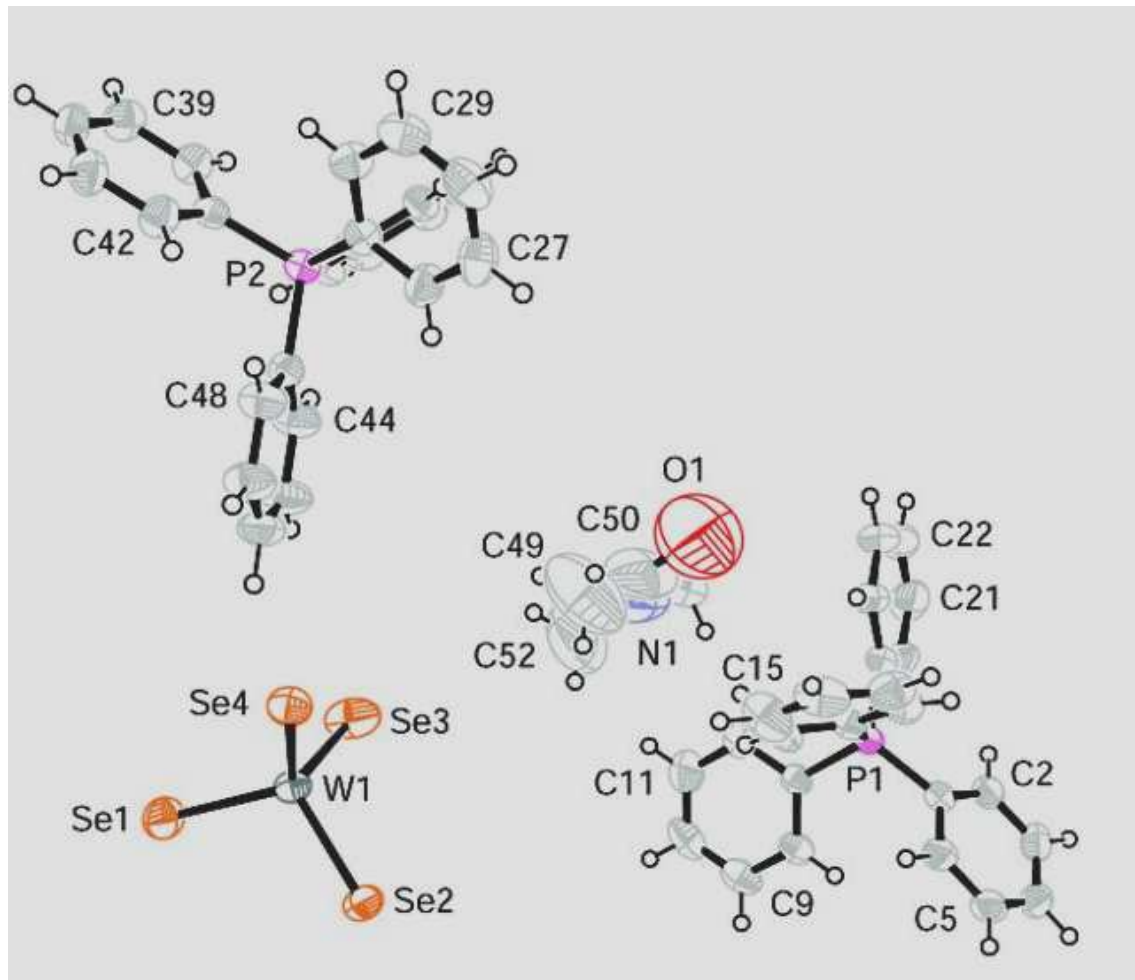


Fig. 10. Crystal Structure of $[\text{PPh}_4]_2[\text{WSe}_4]\bullet\text{DMA}$ [1]

Table 2. Crystallographic Detail of [1]

Empirical formula	C ₅₂ H ₄₉ N O P ₂ Se ₄ W		
Formula weight	1265.55		
Temperature	200(2) K		
Wavelength	1.54178 Å		
Crystal system, space group	Monoclinic, P2 ₁ /c		
Unit cell dimensions	a = 12.6127(5) Å	alpha = 90°	
	b = 30.0984(12) Å	beta = 106.524(2)°	
	c = 13.4552(6) Å	gamma = 90°	
Volume	4896.9(4) Å ³		
Z, Calculated density	4, 1.717 Mg/m ³		
Absorption coefficient	8.678 mm ⁻¹		
F(000)	2464		
Crystal size	0.22 x 0.10 x 0.06 mm		
Theta range for data collection	2.94 to 68.88°		
Limiting indices	-15 ≤ h ≤ 15, -34 ≤ k ≤ 34, -13 ≤ l ≤ 15		
Reflections collected / unique	54565 / 8422 [R(int) = 0.0425]		
Completeness to theta	= 68.88° 92.6 %		
Absorption correction	Semi-empirical from equivalents		
Max. and min. transmission	0.6240 and 0.2512		
Refinement method	Full-matrix least-squares on F ²		
Data / restraints / parameters	8422 / 0 / 553		
Goodness-of-fit on F ²	1.095		
Final R indices [I>2sigma(I)]	R1 = 0.0342, wR2 = 0.0667		
R indices (all data)	R1 = 0.0477, wR2 = 0.0713		
Largest diff. peak and hole	0.683 and -0.762 eÅ ⁻³		

Table 3. Bond lengths [Å] and angles [°] for the [WSe₄]²⁻ anion of [1].

W(1)-Se(3)	2.3032(6)	Se(3)-W(1)-Se(4)	108.49(2)
W(1)-Se(4)	2.3042(5)	Se(3)-W(1)-Se(2)	110.09(2)
W(1)-Se(2)	2.3228(5)	Se(4)-W(1)-Se(2)	109.35(2)
W(1)-Se(1)	2.3278(6)	Se(3)-W(1)-Se(1)	109.94(3)
		Se(4)-W(1)-Se(1)	109.19(2)
		Se(2)-W(1)-Se(1)	109.77(2)

Average W-Se Bond Distance (Å): **2.3145**Average Se-W-Se Bond Angle (°): **109.47**

The data obtained shows the expected tetrahedral geometry of the [WSe₄]²⁻ unit, where the average angle formed between two selenium atoms and the tungsten atom is 109.47°; which is very close to the angle shown for ideal tetrahedral geometries, 109.5° (see Table 3). The average distance between tungsten and selenium atoms in this uncoordinated unit is 2.3145 Å, and all these bond distances are within 0.02 Å of each

other. The data shown in Table 3 can be compared with the parameters obtained by Kolis *et al.* when they first synthesized the $[\text{WSe}_4]^{2-}$ unit.⁶ These specific parameters are shown in Table 4.

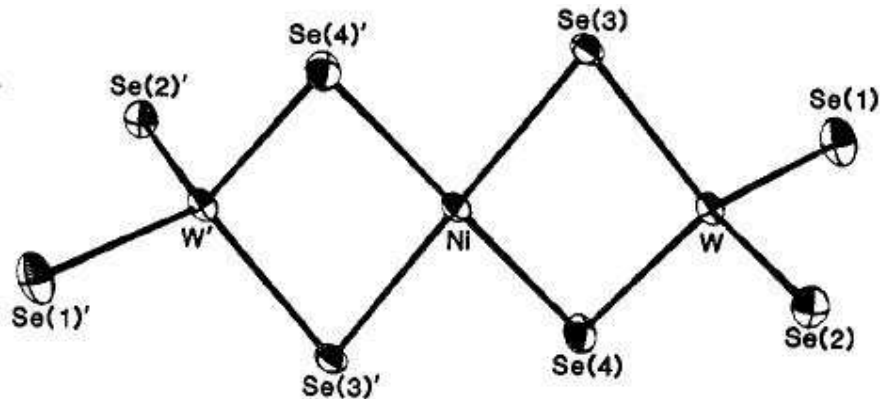
Table 4. Bond lengths [\AA] and angles [$^\circ$] for the $[\text{WSe}_4]^{2-}$ anion obtain by *Kolis et al.*⁶ This anion is analogous to the one shown in [1]. (Atoms not shown are related by symmetry)

W(1)-Se(2)	2.316(1)	Se(1)-W(1)-Se(1)	110.5(1)
W(1)-Se(1)	2.314(1)	Se(2)-W(1)-Se(2)	110.7(1)
		Se(2)-W(1)-Se(1)	109.4(1)
Average W-Se Bond Distance (\AA): 2.315		Average Se-W-Se Bond Angle ($^\circ$): 110.2	

Overall, both sets of data are similar; however, it is worth noticing that the crystallographic data of [1] has less uncertainty. The Se-W-Se bond angles obtained for [1] also are closer to tetrahedral; having an average bond angle of 109.45° (Table 3) while the structure synthesized by Kolis *et al.* has an average Se-W-Se bond angle of 110.2° (Table 4). This angle is 0.7° larger than the ideal angle for tetrahedral structures whereas the average bond angle for [1] is only 0.01 \AA less than the ideal value. The average W-Se bond distances for both structures are approximately equal.

The bond distances between W and Se atoms observed in [1] can also be compared with the bond distances in $[\text{WSe}_4]^{2-}$ units that exist in coordination with late transition-metals. One of these structures is the compound with the formula $[\text{PPh}_4]_2[\text{Ni}(\text{WSe}_4)_2]$ reported by Ansari *et al.* (see Figure 11). The bond distances between the W and Se atoms in this structure vary more and are only within 0.07 \AA of each other, about three times more variation than in the uncoordinated $[\text{WSe}_4]^{2-}$ unit in [1]. The Se-W-Se bond angles in this coordinated unit also show an adjustment in which one of the angles is notably smaller than the rest, (Se(3)-W-Se(4), 103.62°). The coordinated

$[\text{WSe}_4]^{2-}$ still shows a near tetrahedral geometry, however it allows the Ni atom to be nearly square planar, by reducing one of its Se-W-Se angles and increasing the rest of the bond angles to more than 109.5° .



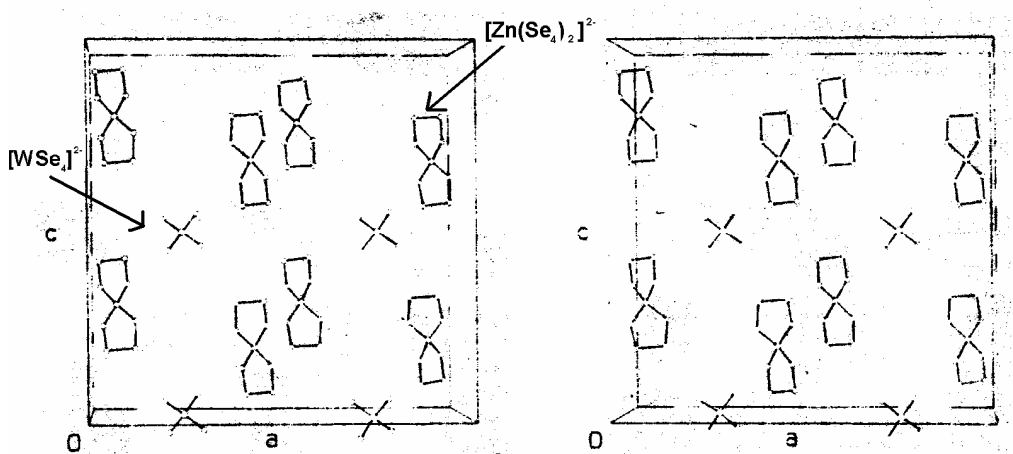
W-Se(1)	2.277(1)	Se(3)-W(1)-Se(4)	103.62(3)
W-Se(2)	2.285(1)	Se(3)-W(1)-Se(2)	110.75(3)
W-Se(3)	2.350(1)	Se(4)-W(1)-Se(2)	110.81(3)
W-Se(4)	2.347(1)	Se(3)-W(1)-Se(1)	110.14(3)
		Se(4)-W(1)-Se(1)	111.22(3)
		Se(2)-W(1)-Se(1)	110.15(3)

Average W-Se Bond Distance (\AA): **2.315**

Average Se-W-Se Bond Angle ($^\circ$): **109.45**

Fig. 11; Bond distances [\AA] and angles [$^\circ$] of $[\text{WSe}_4]^{2-}$ in $[\text{PPh}_4]_2[\text{Ni}(\text{WSe}_4)_2]$

The $[\text{WSe}_4]^{2-}$ unit present in the $(\text{PPh}_4)_6[\text{Zn}(\text{Se}_4)_2]_2[\text{WSe}_4]$ compound reported by Neumüller and coworkers can also be compared with the $[\text{WSe}_4]^{2-}$ unit in [1].¹³ In this case the $[\text{WSe}_4]^{2-}$ is not directly coordinated to the late transition-metal, which explains why none of the bond angles are more than 1 degree from the 109.5° value. Also, the bond distances of the W and the Se atoms differ only 0.01 \AA from each other. As expected, the $[\text{WSe}_4]^{2-}$ unit in this compound is more similar to that in [1] than to the $[\text{WSe}_4]^{2-}$ unit coordinated to a Ni^{2+} in Figure 11.



W-Se(9) 2.297(4)
W-Se(10) 2.311(4)

Se(9)-W-Se(9') 109.4(1)
Se(9)-W-Se(10) 108.7(1)
Se(9)-W-Se(10') 110.1(1)
Se(10)-W-Se(10') 109.7(1)

Average W-Se Bond Distance (\AA): **2.304**

Average Se-W-Se Bond Angle ($^\circ$): **109.5**

Fig. 12; $(\text{PPh}_4)_6[\text{Zn}(\text{Se}_4)_2]_2[\text{WSe}_4]$ structure, bond distances and angles of the $[\text{WSe}_4]^{2-}$ unit.¹³ (PPh_4 not shown for clarity)

Besides the structure of the tetrahedral $[\text{WSe}_4]^{2-}$ unit, [1] shows the structure of the two tetraphenylphosphonium ions present in the compound and a DMA molecule as part of the crystal unit. The counterions and the tetraselenotungstate unit exist in relatively fixed position within the unit, which is evidenced by the small size and nearly-spherical shape of the ellipsoids representing their atoms. However, the carbon, oxygen, and nitrogen atoms in DMA are represented by large ellipsoids, which do not show a very spherical shape. These can be explained by two main factors. First, these atoms could have higher vibration within the crystal unit, and second, the DMA molecule may have some disorder. DMA was used as the solvent when attempting the synthesis of new transition-metal selenides. DMA may be disordered within the crystal; as this molecule may be able to freely move within the pocket that exists between the two counter ions and the tetraselenotungstate units.

Conclusion

A variety of transition-metals were reacted with tetraselenometalate anions and triphenylphosphine in attempts to grow crystals suitable for X-ray diffraction studies. The use of acetonitrile as the reaction solvent had more tendency to encourage the formation of a precipitate, but not crystals. Crystals were more likely obtained by dissolving the reagents in DMA and layering with THF. Sometimes ether had to be used, in addition to THF, in the layering process to aid their formation. Even though there is some spectroscopic evidence that novel compounds were synthesized, no new compounds have been completely characterized up till now. Crystals of some of the reaction products were obtained, however, some were too fragile or unstable which made them unsuitable for X-ray crystallography. Crystals that show stability were collected and were sent to the College of William and Mary to attempt a successful structure determination of novel compounds. New methods of crystal growth could be used in the future as well as new transition metal and phosphine ligands to study the syntheses of novel complexes.

A new crystal structure with the formula $[PPh_4]_2[WSe_4] \bullet DMA$ was characterized by X-ray crystallography. Comparisons between the uncoordinated $[WSe_4]^{2-}$ unit in this structure, and $[WSe_4]^{2-}$ in other structures, both uncoordinated and coordinated to a transition-metal, show that when bonded to a metal there is a notable adjustment in Se-W-Se bond angles and the W-Se bond distances tend to vary approximately three times more than in the free $[WSe_4]^{2-}$ unit.

Experimental

Syntheses. All syntheses were performed in oven-dried glassware under a purified nitrogen or argon atmosphere using standard Schlenk techniques and an MBraun Labmaster 130 Glove box (under N₂). Commercially available compounds were used without further purification, unless noted otherwise. Solvents were dried by the following methods: DMA distilled under reduced pressure (water aspirator) from calcium hydride, THF distilled from sodium/benzonphenone under nitrogen, and acetonitrile distilled from calcium hydride. Reaction mixtures were cooled to approximately -20°C in a conventional freezer. Infrared spectra were obtained using a Fourier-Transform Thermo Electron IR 100 infrared spectrophotometer. UV-visible spectra were recorded on a Cary Bio 50 UV-vis spectrophotometer with DMA as a solvent. Na₂Se₃, (PPh₄)₂(WSe₄) and (PPh₄)₂(MoSe₄) were prepared by slight variations of literature procedures.⁶

Crystals were grown by layering THF (and in some cases diethyl ether) over a DMA solution of the respective compounds in a Schlenk flask at room temperature under an atmosphere of N₂. In the later stages of the study, suitable crystals were mounted into a glass capillaries inside of a glove bag (see Figure 13). Vacuum grease was used as the adhesive medium. X-ray crystallographic studies were done with a Bruker SMART APEX II: 4K CCD System with 3-circle goniometer, Oxford Cryostream Plus variable temp. system (80-500 K).

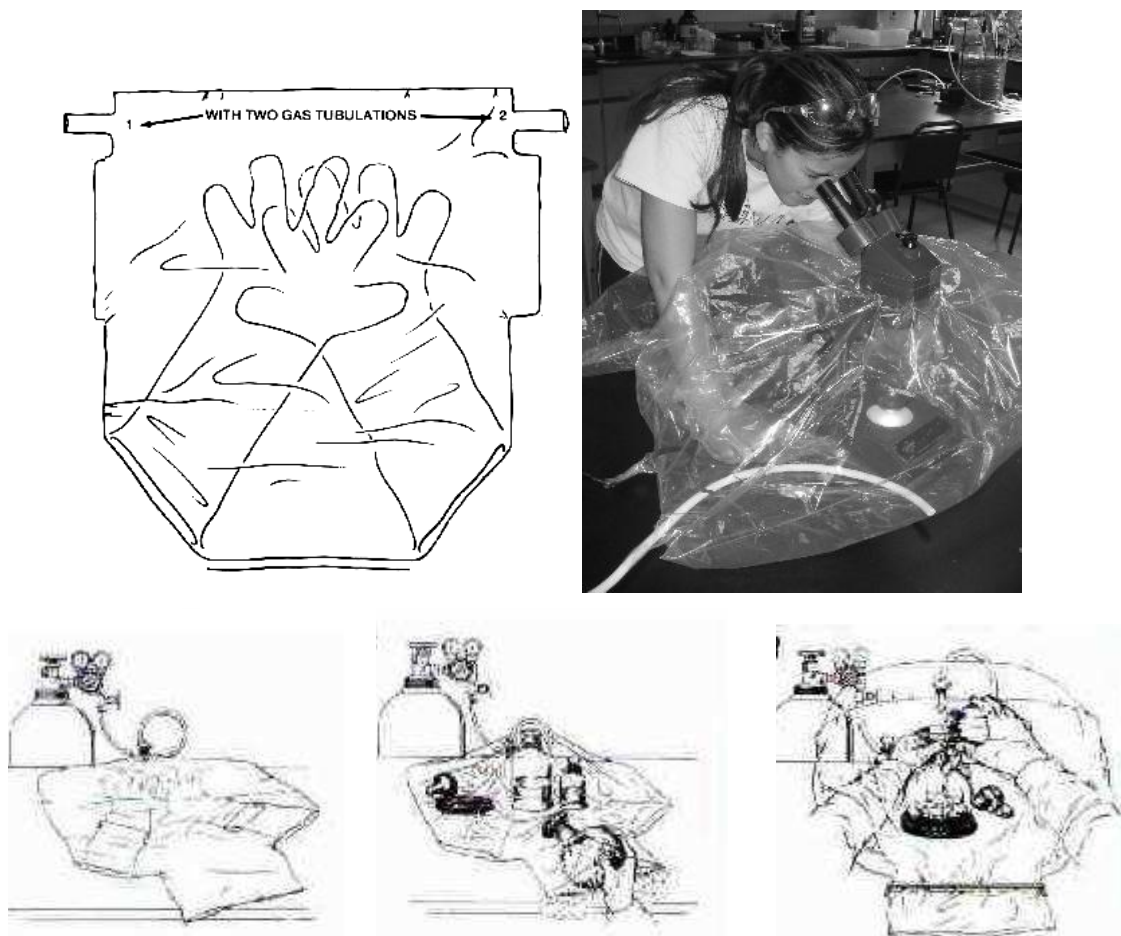


Fig. 13. The Glove Bag (use for crystal mounting into capillaries)¹⁴

Synthesis of Na₂Se₃.



Solid sodium (1.50 g; 65.2 mmol) was placed in a three neck round bottom flask previously purged with an inert gas (Ar) and containing a stirring bar. The flask was immersed in a slush bath containing dry ice and isopropyl alcohol. The flask also had a condenser, previously purged with argon, in which the slush mixture could be placed (the complete set up for this reaction is shown in Figure 4). Ammonia gas was then allowed to condense into the flask in order to dissolve the sodium metal. After the sodium was

completely dissolved, selenium powder (7.73 g; 97.9 mmol) was introduced into the flask under argon. More ammonia was allowed to condense into the flask to assure that the reagents could mix well and, after letting the reaction stir for approximately an hour, argon gas was passed through with the purpose of removing the ammonia and drying the final product. The reaction vessel was then taken into the glove box and the dry powder was scraped out of the container. The product had a dark gray color and it was kept inside of the glove box for future use. (7.24 g; 25.5 mmol, 79.5% yield).

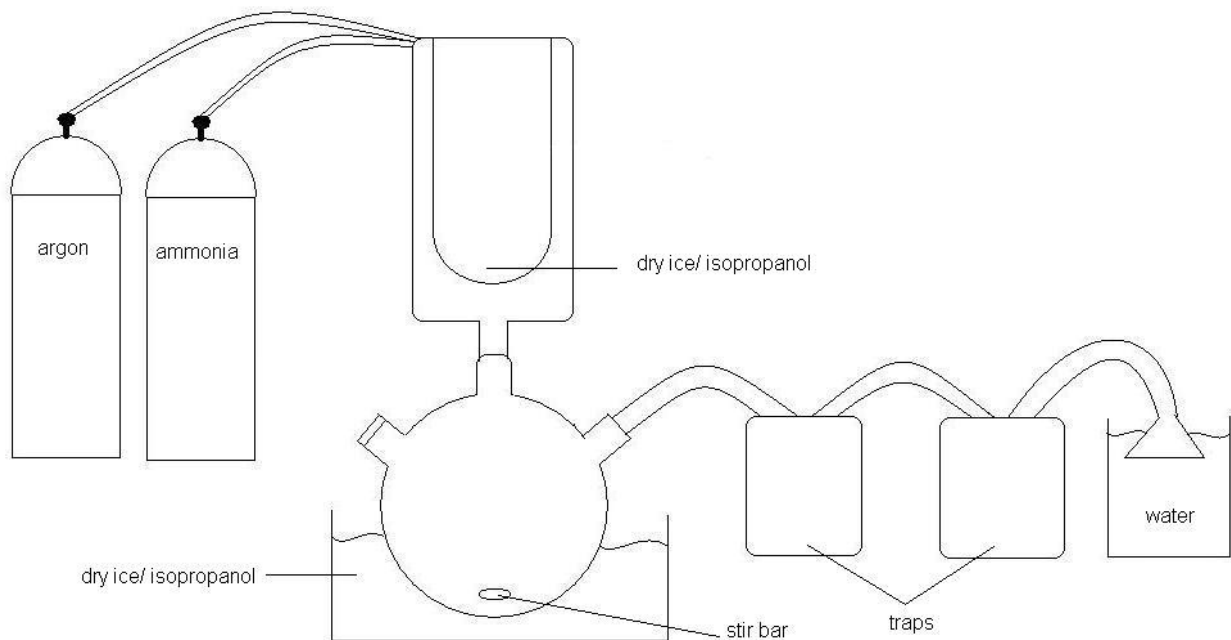
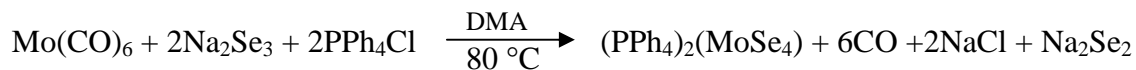


Fig. 14. Reaction set up for the syntheses of Na_2Se_4

Synthesis of $(\text{PPh}_4)_2(\text{MoSe}_4)$.



Solid Na_2Se_3 (0.259 g, 0.917 mmol), molybdenum hexacarbonyl, $\text{Mo}(\text{CO})_6$ (0.242 g, 0.917 mmol), and tetraphenylphosphonium bromide PPh_4Br (0.769 g, 1.83

mmol) were weighed into a 100-mL Schlenk flask. The reagents were dissolved in DMA while in the Schlenk line. The solution was then heated to 80 °C for at least 3 hours and left stirring overnight. The reaction was then layered with 20 mL of freshly distilled tetrahydrofuran (THF), and, after storage at -20 °C overnight, the solution was filtered in the Schlenk line as indicated in Figure 5, and the product was washed with ether before being isolated. The precipitate obtained was blue, as previously reported by Kolis and coworkers (0.499 g, 45.8 mmol, 49.5% yield): IR 1630, 1433, 1103 cm⁻¹;

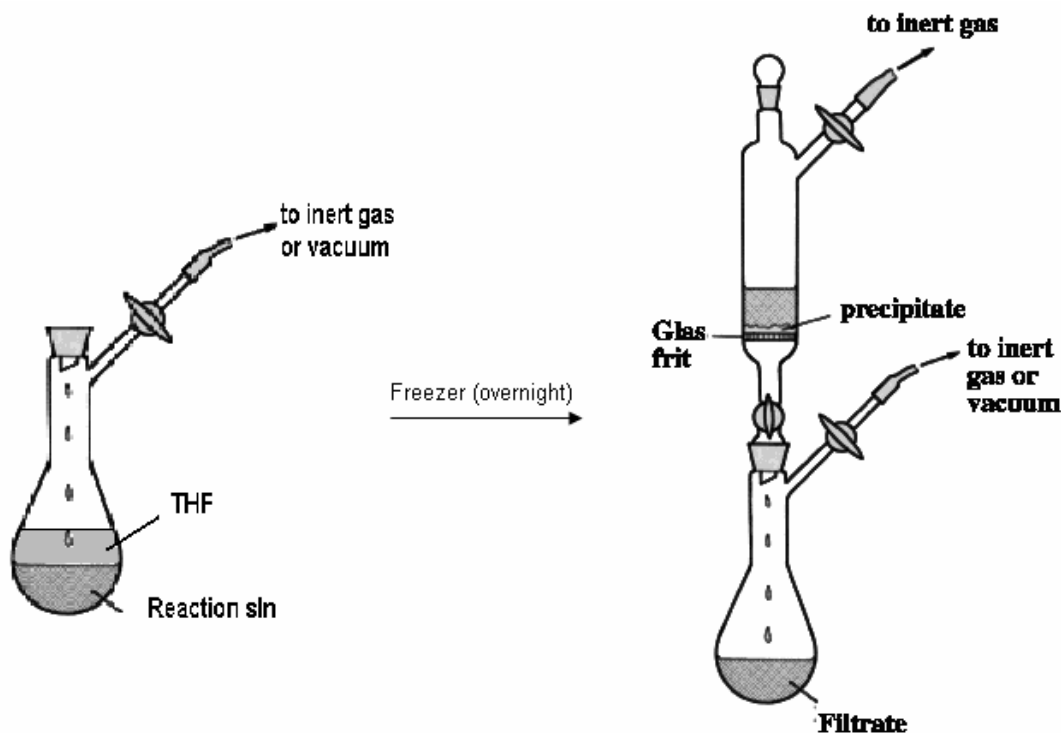
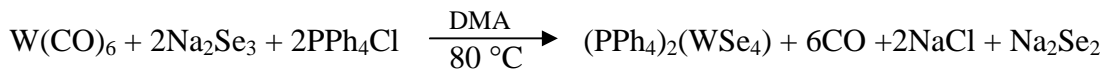


Fig. 15. Layering and filtration procedure used to collect the products of the tetraselenometalates' reactions

Synthesis of $(\text{PPh}_4)_2(\text{WSe}_4)$.



The method is the same as the previous compound but employing Na₂Se₃ (0.240 g, 0.849 mmol), tungsten hexacarbonyl W(CO)₆ (0.299 g, 0.849 mmol), and tetraphenylphosphonium bromide PPh₄Br (0.712 g, 1.70 mmol). The precipitate obtained after filtration was red, as previously reported by Kolis *et al.* (0.645 g; 54.7 mol; 64.5% yield). IR 1631, 1434, 1104 cm⁻¹

Reaction product of (PPh₄)₂(WSe₄), Pt²⁺, and PPh₃ in DMA.



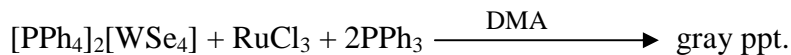
Solid tetraphenylphosphonium tetraselenotungstate (PPh₄)₂(WSe₄) (0.104 g, 0.0882 mmol), platinum (II) chloride, PtCl₂ (0.048 g, 0.18 mmol), and triphenylphosphine, PPh₃, (0.096 g, 0.37 mmol) were weighed into a 100-mL Schlenk flask. 10 mL of dry DMA were added under N₂ at room temperature. After stirring for 20 min, the solution turned dark red. The solution was stirred for a minimum of three hours, then layered with 20 mL of freshly distilled THF, and cooled overnight in the freezer at -20 °C. After filtration no precipitate was successfully obtained. 25 mL of anhydrous ether were added to the filtrate and the solution was place in the freezer to cool overnight. Precipitate was obtained after filtering the solution, however, dark orange-brown crystal were left behind on the walls of the Schlenk flask. The crystals could not be successfully collected. The precipitate obtained was dark gray. IR (precipitate) 1433, 1091 cm⁻¹.

Reaction product of (PPh₄)₂(MoSe₄), Pt²⁺, and PPh₃ in DMA.



The method was the same as in compound 4, but employing tetraphenylphosphonium tetraselenomolybdate ($\text{PPh}_4)_2(\text{MoSe}_4)$ (0.104 g, 0.0882 mmol), platinum (II) chloride PtCl_2 (0.048 g, 0.18 mmol), and triphenylphosphine PPh_3 (0.096 g, 0.37 mmol). The crystals left behind in the Schlenk flask had a brown/orange color and could not be collected. The precipitate was tan. IR 1049 cm^{-1} .

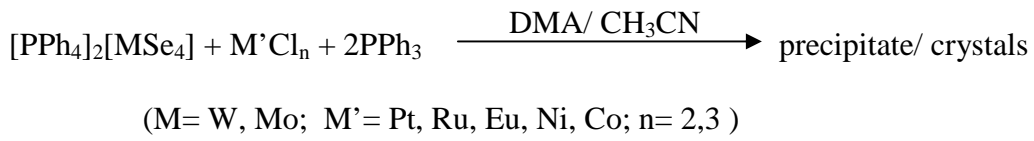
Reaction product of $(\text{PPh}_4)_2(\text{WSe}_4)$, Ru^{3+} , and PPh_3 in DMA.



The procedure used was the same as in the previous compound but employing tetraphenylphosphonium tetraselenotungstate ($\text{PPh}_4)_2(\text{WSe}_4)$ (0.104 g, 0.0882 mmol), ruthenium (III) chloride RuCl_3 (0.048 g, 0.18 mmol), and triphenylphosphine PPh_3 (0.096 g, 0.37 mmol). The precipitate obtained was dark gray. IR (precipitate) 1434, 1105 cm^{-1} .

All the reactions products of the tetraselenometallate anions with transition-metal chloride salts (except for products 4, 5, and 7) follow the same general procedure: The specific reagents were weighed into a 100-mL Schlenk flask inside of the glove box. 10 mL of either DMA or acetonitrile were added to the flasks to dissolve the reagents. The solutions were left stirring overnight. Then, they were layered with 20 mL of tetrahydrofuran (THF) and place in the freezer at 4°C overnight to encourage crystal growth. The reactions were filtered (Figure. 5) and washed with 5 mL of anhydrous ether

to ensure that the reaction products were completely dry. Then, the flasks were taken into the glove box where the products were collected and stored in screw cap vials. IR and UV-vis spectra were taken whenever possible.



Reaction product of $(\text{PPh}_4)_2(\text{WSe}_4)$, Co^{2+} , and PPh_3 in CH_3CN . Product obtained from tetraphenylphosphonium tetraselenotungstate (0.120 g; 0.102 mmol), cobalt (II) chloride, (0.0280 g; 0.216 mmol) and triphenylphosphine (0.105 g; 0.400 mmol). 23 mg of a gray precipitate were recovered. IR 1437, 1259, 1092, 1014 cm^{-1} .

Reaction products of $(\text{PPh}_4)_2(\text{WSe}_4)$, Ru^{3+} , and PPh_3 in CH_3CN . Product obtained from tetraphenylphosphonium tetraselenotungstate (0.105 g; 0.0891 mmol), ruthenium (III) chloride, (0.045 g; 0.183 mmol) and triphenylphosphine (0.091 g; 0.347 mmol). 38 mg of gray precipitate were recovered. Yellow crystals with needle shape were also formed. IR 1435, 1107 cm^{-1} .

Reaction product of $(\text{PPh}_4)_2(\text{MoSe}_4)$, Co^{2+} , and PPh_3 in CNCH_3 . Product obtained from tetraphenylphosphonium tetramolybdate (0.100 g; 0.0917 mmol), cobalt (II) chloride, (0.0240 g; 0.169 mmol) and triphenylphosphine (0.096 g; 0.366 mmol). 28 mg of gray precipitate were recovered.

Reaction product of $(PPh_4)_2(WSe_4)$, Ni^{2+} , and PPh_3 in CH_3CN . Product obtained from tetraphenylphosphonium tetraselenotungstate (0.103 g; 0.0873 mmol), nickel (II) chloride, (0.022 g; 0.170 mmol) and triphenylphosphine (0.090 g; 0.343 mmol). 45 mg of pale pink precipitate were recovered. IR 1435, 1106 cm^{-1} .

Reaction product of $(PPh_4)_2(MoSe_4)$, Ni^{2+} , and PPh_3 in DMA. Product obtained from tetraphenylphosphonium tetraselenomolybdate (0.100 g; 0.0917 mmol), nickel (II) chloride, (0.0240 g; 0.185 mmol) and triphenylphosphine (0.090 g; 0.343 mmol). 28 mg of a pale yellow precipitate were recovered. IR 1433, 1105 cm^{-1} .

Reaction product of $(PPh_4)_2(WSe_4)$, Ni^{2+} , and PPh_3 in DMA. Product obtained from tetraphenylphosphonium tetraselenotungstate (0.100 g; 0.0848 mmol), nickel (II) chloride, (0.022 g; 0.170 mmol) and triphenylphosphine (0.090 g; 0.343 mmol). 33 mg of red crystals were recovered. IR 1433, 1104 cm^{-1} .

Reaction product of $(PPh_4)_2(MoSe_4)$, Co^{2+} , and PPh_3 in DMA. Product obtained from tetraphenylphosphonium tetraselenomolybdate (0.100 g; 0.0917 mmol), cobalt (II) chloride, (0.024 g; 0.169 mmol) and triphenylphosphine (0.089 g; 0.339 mmol). 35 mg of a turquoise precipitate were recovered. IR 1607, 1106 cm^{-1} .

Reaction product of $(PPh_4)_2(WSe_4)$, Sm^{3+} , and PPh_3 in DMA. Product obtained from tetraphenylphosphonium tetraselenotungstate (0.100 g; 0.0848 mmol), samarium (III) chloride, (0.044 g; 0.171 mmol) and triphenylphosphine (0.089 g; 0.339 mmol). Red

crystals were recovered. IR 1605, 1433, 1105 cm⁻¹.

Reaction product of (PPh₄)₂(MoSe₄), Sm³⁺, and PPh₃ in DMA. Product obtained from tetraphenylphosphonium tetraselenomolybdate (0.100 g; 0.0917 mmol), samarium (III) chloride, (0.047 g; 0.183 mmol) and triphenylphosphine (0.090 g; 0.343 mmol). Blue crystals were recovered. IR 1608, 1434, 1104 cm⁻¹.

Reaction product of (PPh₄)₂(WSe₄), Tb³⁺, and PPh₃ in DMA. Product obtained from tetraphenylphosphonium tetraselenotungstate (0.102 g; 0.0866 mmol), terbium (III) chloride, (0.045 g; 0.170 mmol) and triphenylphosphine (0.090 g; 0.343 mmol). Red crystals were recovered.

Reaction product of (PPh₄)₂(WSe₄), Eu³⁺, and PPh₃ in DMA. Product obtained from tetraphenylphosphonium tetraselenotungstate (0.100 g; 0.0848 mmol), europium (III) chloride, (0.038 g; 0.147 mmol) and triphenylphosphine (0.090 g; 0.343 mmol). 32 mg of red precipitate was recovered. IR 1607, 1434, 1105 cm⁻¹.

Reaction product of (PPh₄)₂(WSe₄), Zn²⁺, and PPh₃ in CH₃CN. Product obtained from tetraphenylphosphonium tetraselenotungstate (0.100 g; 0.0848 mmol), zinc (II) chloride, (0.023 g; 0.167 mmol) and triphenylphosphine (0.090 g; 0.343 mmol). Light brown precipitate was recovered as well as dark green crystals. IR 1434, 1259, 1106, 1016, 795, 720, 686 cm⁻¹

Reaction product of $(PPh_4)_2(MoSe_4)$, Cr^{3+} , and PPh_3 in DMA. Product obtained from tetraphenylphosphonium tetraselenomolybdate (0.103 g; 0.0944 mmol), chromium (III) chloride, (0.042 g; 0.182 mmol) and triphenylphosphine (0.099 g; 0.377 mmol). A black precipitate was recovered.

Reaction product of $(PPh_4)_2(WSe_4)$, Cr^{3+} , and PPh_3 in CH_3CN . Product obtained from tetraphenylphosphonium tetraselenotungstate (0.100 g; 0.0848 mmol), chromium (III) chloride, (0.042 g; 0.182 mmol) and triphenylphosphine (0.092 g; 0.351 mmol). A black precipitate was recovered. IR 1435, 1106 cm^{-1}

Reaction product of $(PPh_4)_2(MoSe_4)$, Tb^{3+} , and PPh_3 in DMA. Product obtained from tetraphenylphosphonium tetraselenomolybdate (0.102 g; 0.0935 mmol), terbium (III) chloride, (0.049 g; 0.185 mmol) and triphenylphosphine (0.090 g; 0.343 mmol). Red crystals were recovered.

Reaction product of $(PPh_4)_2(WSe_4)$, Fe^{2+} , and PPh_3 in CH_3CN . Product obtained from tetraphenylphosphonium tetraselenotungstate (0.100 g; 0.0848 mmol), iron (II) chloride, (0.042 g; 0.174 mmol) and triphenylphosphine (0.092 g; 0.351 mmol). A dark brown precipitate was recovered.

Reaction product of $(PPh_4)_2(WSe_4)$, Eu^{3+} , and PPh_3 in CH_3CN . Product obtained from tetraphenylphosphonium tetraselenotungstate (0.100 g; 0.0848 mmol), europium

(III) chloride, (0.038 g; 0.147 mmol) and triphenylphosphine (0.090 g; 0.343 mmol). 32 mg of red precipitate was recovered.

Future Work

Other potential aspects of our study were to vary the phosphine ligand present in the synthesis as well as the methods for attempting crystal growth. However, the compounds reported here were all synthesized with triphenylphosphine (PPh_3). In the future, the syntheses of new compounds could be studied with the addition of other ligands other than PPh_3 , like diphenylphosphinoethane (dppe) shown in Figure 16. The use of this particular bidentate ligand may give rise to new interesting geometries of the new selenide compounds of interest.

Other crystal growth methods, like diffusion tubes and other methods involving vapor diffusion, previously used in our lab could be employed to attempt the growth of more stable crystals suitable for X-ray crystallographic studies.¹⁵ In addition, it is also planned for the future to study the reactions chemistry of the new soluble transition-metal selenides by ^{77}Se , ^{95}Mo , ^{183}Mo , and ^{31}P NMR spectroscopies.

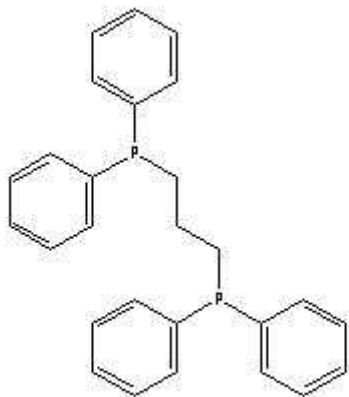


Fig 16. dppe structure, $\text{Ph}_2\text{PCH}_2\text{CH}_2\text{PPh}_2$

Acknowledgements

We are grateful to Dr. Robert Pike at the College of William and Mary for providing crystallographic data. We also thank Dr. Margaret Kastner of Bucknell University and Dr. Hoseop Yun of Anjou University (South Korea) for accepting crystals for analysis. We also acknowledge the Lycoming College Chemistry faculty and the past students working in this research.

References

- ¹ Ansari, M.; Ibers, J.; “Soluble Selenides and Tellurides” *Coord. Chem Rev.*, **1990**, *100*, 223-266
- ² Alberty, R.; “Thermodynamics of the Mechanism of the Nitrogenase Reaction,” *Biophys. Chem.*, **2005**, *114*, 115-120.
- ³ Sanders, A.; Jong, A.; de Beer, V.; van Veen, J.; Niemantsverdriet, J., “Formation of Cobalt-Molybdenum Sulfides in Hydro Treating Catalyst: a Surface Science Approach” *Appl. Surf. Sci.*, **1999**, *144*, 380-384.
- ⁴ Zhang, Q.-F.; Leung, W.-H.; Xin, X., “Heteroselenometallic Cluster Compounds with Tetraselenometallates” *Coord. Chem. Rev.*, **2002**, *224*, 35-49.
- ⁵ Kolis, J.; Roof, L., “New Developments in the Coordination Chemistry of Inorganic Selenide and Telluride Ligands” *Chem. Rev.*, **1993**, *93*, 1037-1080.
- ⁶ O’Neal, S.; Kolis, J., “Convenient Preparation and Structures of Selenometallates

MoSe_4^{-2} WSe_4^{-2} and MoSe_9^{-2} from Polyselenide Anions and Metal Carbonyls" *J. Am. Chem. Soc.* **1988**, *110*, 1971-1973

⁷ Müller, A.; Diemann, E.; Joster, R.; Bögge, H., "Transition-Metal Thiometalates: Properties and Significance in Complex and Bioinorganic Chemistry" *Angew. Chem. Int. Ed. Engl.* **1981**, *20*, 934-955

⁸ Ansari, M.; Chau, C.-N.; Mahler, C.; Ibers, J.; "Mixed-Metal Selenides: Synthesis and Characterization of the $\text{Ni}(\text{Se}_2)(\text{WSe}_4)^{2-}$ and $\text{M}(\text{WSe}_4)_2^{2-}$ ($\text{M} = \text{Ni}, \text{Pd}$) Anions" *Inorg. Chem.*, **1989**, *28*, 650-654.

⁹ Shiffler, Z; Baldwin, S.; Keane, J.; Belz, B; Barr, M.; Slavin III, E.; Kastner, M.; Mahler, C.; "Bis(tetraphenylphosphonium) bis(tetraselenomolybdato)palladate(II)" *Acta. Cryst.*, **2004**, *E60*, 1-3.

¹⁰ Christuk, C.; Ansari, M.; Ibers, J.; "Interactions of Coinage-Group Cations with the Tetraselenotungstate Anion: Multinuclear NMR Spectoscopic Results and Crystal Structure of $(\mu\text{-WSe}_4)[(\text{PMe}_2\text{Ph})_2\text{Cu}]_2$, $(\mu\text{-WSe}_4)[\text{PMePh}_2\text{Au}]_2$, and $(\mu_3\text{-Cl})(\mu_3\text{-WSe}_4)[(\text{PPh}_3)\text{Cu}]_3$ " *Inorg. Chem.*, **1992**, *31*, 4365-4369

¹¹ Zhang, Q.-F; Cao, R.; Hong, M.-C.; Wu, D.; Zhang, W.-J.; Zheng, Y.; Liu, H.-Q., "Syntheses and Spectroscopic Characterization of the Compounds Containing Univalent Coinage and Tetraselenomolybdate. Crystal structure $[\text{MoSe}_4(\text{AuPPh}_3)_2]$ " *Inorg. Chim. Acta.*, **1998**, *271*, 93-98.

¹² Zhang, Q.F. ; Leung, W.H. ; Hong, M.C. ; Kennard, C.; Xin, X.Q.; " Skeleton Atomic Effect in Nonlinear Optical Properties of Linear Trinuclear Heteroselenometallic Compounds with Univalent Coinage Metals" *New. J. Chem.*, **2001**, *25*, 465-470

¹³ Neumüller, B.; Ha-Eierdanz, M; Müller, U; Magull, S; Kräuter, G.; Denhnick, K.,

“Synthese und Kristallstrukturen der Polyselenidokomplexe

(PPh_4)₆[M(Se₄)₂]₂[WSe₄]•DMF mit M= Zink und Quecksilber” *Z. anorg. Allg. Chem.*

1992, 609 12-18

¹⁴ Picture taken from www.i-2-r.com

¹⁵ Mahler, Charles H. personal communication.

Supplementary Material

Table 5. Bond lengths [Å] and angles [°] for [1]

W(1)-Se(3)	2.3032(6)	C(16)-H(16)	0.9500
W(1)-Se(4)	2.3042(5)	C(17)-C(18)	1.377(8)
W(1)-Se(2)	2.3228(5)	C(17)-H(17)	0.9500
W(1)-Se(1)	2.3278(6)	C(18)-H(18)	0.9500
P(1)-C(13)	1.791(5)	C(19)-C(20)	1.381(7)
P(1)-C(1)	1.791(5)	C(19)-C(24)	1.391(7)
P(1)-C(7)	1.793(4)	C(20)-C(21)	1.381(8)
P(1)-C(19)	1.793(5)	C(20)-H(20)	0.9500
P(2)-C(31)	1.795(4)	C(21)-C(22)	1.377(10)
P(2)-C(25)	1.798(4)	C(21)-H(21)	0.9500
P(2)-C(43)	1.799(5)	C(22)-C(23)	1.351(9)
P(2)-C(37)	1.803(5)	C(22)-H(22)	0.9500
C(49)-C(50)	1.45(2)	C(23)-C(24)	1.385(8)
C(49)-H(49A)	0.9800	C(23)-H(23)	0.9500
C(49)-H(49B)	0.9800	C(24)-H(24)	0.9500
C(49)-H(49C)	0.9800	C(25)-C(30)	1.376(6)
N(1)-C(50)	1.186(19)	C(25)-C(26)	1.387(6)
N(1)-C(51)	1.340(19)	C(26)-C(27)	1.382(7)
N(1)-C(52)	1.403(14)	C(26)-H(26)	0.9500
C(1)-C(2)	1.380(6)	C(27)-C(28)	1.365(8)
C(1)-C(6)	1.395(6)	C(27)-H(27)	0.9500
C(2)-C(3)	1.378(7)	C(28)-C(29)	1.367(8)
C(2)-H(2)	0.9500	C(28)-H(28)	0.9500
C(3)-C(4)	1.387(7)	C(29)-C(30)	1.386(7)
C(3)-H(3)	0.9500	C(29)-H(29)	0.9500
C(4)-C(5)	1.373(8)	C(30)-H(30)	0.9500
C(4)-H(4)	0.9500	C(31)-C(36)	1.390(6)
C(5)-C(6)	1.375(7)	C(31)-C(32)	1.393(6)
C(5)-H(5)	0.9500	C(32)-C(33)	1.374(7)
C(6)-H(6)	0.9500	C(32)-H(32)	0.9500
C(7)-C(12)	1.379(7)	C(33)-C(34)	1.367(7)
C(7)-C(8)	1.388(6)	C(33)-H(33)	0.9500
C(8)-C(9)	1.375(7)	C(34)-C(35)	1.374(7)
C(8)-H(8)	0.9500	C(34)-H(34)	0.9500
C(9)-C(10)	1.363(8)	C(35)-C(36)	1.385(7)
C(9)-H(9)	0.9500	C(35)-H(35)	0.9500
C(10)-C(11)	1.369(9)	C(36)-H(36)	0.9500
C(10)-H(10)	0.9500	C(37)-C(38)	1.377(6)
C(11)-C(12)	1.386(8)	C(37)-C(42)	1.396(7)
C(11)-H(11)	0.9500	C(38)-C(39)	1.387(7)
C(12)-H(12)	0.9500	C(38)-H(38)	0.9500
C(13)-C(14)	1.386(7)	C(39)-C(40)	1.366(7)
C(13)-C(18)	1.387(7)	C(39)-H(39)	0.9500
C(14)-C(15)	1.386(8)	C(40)-C(41)	1.376(7)
C(14)-H(14)	0.9500	C(40)-H(40)	0.9500
C(15)-C(16)	1.364(9)	C(41)-C(42)	1.385(7)
C(15)-H(15)	0.9500	C(41)-H(41)	0.9500
C(16)-C(17)	1.371(9)	C(42)-H(42)	0.9500

Table 5. (Continuation) Bond lengths [Å] and angles [°] for [1]

C(43)-C(44)	1.376(7)	C(2)-C(3)-H(3)	119.9
C(43)-C(48)	1.385(6)	C(4)-C(3)-H(3)	119.9
C(44)-C(45)	1.387(7)	C(5)-C(4)-C(3)	119.9(5)
C(44)-H(44)	0.9500	C(5)-C(4)-H(4)	120.1
C(45)-C(46)	1.371(8)	C(3)-C(4)-H(4)	120.1
C(45)-H(45)	0.9500	C(4)-C(5)-C(6)	120.2(5)
C(46)-C(47)	1.354(8)	C(4)-C(5)-H(5)	119.9
C(46)-H(46)	0.9500	C(6)-C(5)-H(5)	119.9
C(47)-C(48)	1.378(7)	C(5)-C(6)-C(1)	120.3(5)
C(47)-H(47)	0.9500	C(5)-C(6)-H(6)	119.8
C(48)-H(48)	0.9500	C(1)-C(6)-H(6)	119.8
O(1)-C(50)	1.381(16)	C(12)-C(7)-C(8)	119.5(4)
C(51)-H(51A)	0.9800	C(12)-C(7)-P(1)	119.5(4)
C(51)-H(51B)	0.9800	C(8)-C(7)-P(1)	121.0(4)
C(51)-H(51C)	0.9800	C(9)-C(8)-C(7)	119.7(5)
C(52)-H(52A)	0.9800	C(9)-C(8)-H(8)	120.1
C(52)-H(52B)	0.9800	C(7)-C(8)-H(8)	120.1
C(52)-H(52C)	0.9800	C(10)-C(9)-C(8)	121.0(5)
		C(10)-C(9)-H(9)	119.5
Se(3)-W(1)-Se(4)	108.49(2)	C(8)-C(9)-H(9)	119.5
Se(3)-W(1)-Se(2)	110.09(2)	C(9)-C(10)-C(11)	119.6(5)
Se(4)-W(1)-Se(2)	109.35(2)	C(9)-C(10)-H(10)	120.2
Se(3)-W(1)-Se(1)	109.94(3)	C(11)-C(10)-H(10)	120.2
Se(4)-W(1)-Se(1)	109.19(2)	C(10)-C(11)-C(12)	120.7(6)
Se(2)-W(1)-Se(1)	109.77(2)	C(10)-C(11)-H(11)	119.7
C(13)-P(1)-C(1)	107.4(2)	C(12)-C(11)-H(11)	119.7
C(13)-P(1)-C(7)	110.0(2)	C(7)-C(12)-C(11)	119.6(5)
C(1)-P(1)-C(7)	108.5(2)	C(7)-C(12)-H(12)	120.2
C(13)-P(1)-C(19)	108.9(2)	C(11)-C(12)-H(12)	120.2
C(1)-P(1)-C(19)	114.0(2)	C(14)-C(13)-C(18)	118.8(5)
C(7)-P(1)-C(19)	108.0(2)	C(14)-C(13)-P(1)	121.6(4)
C(31)-P(2)-C(25)	108.8(2)	C(18)-C(13)-P(1)	119.6(4)
C(31)-P(2)-C(43)	110.8(2)	C(13)-C(14)-C(15)	120.0(5)
C(25)-P(2)-C(43)	107.6(2)	C(13)-C(14)-H(14)	120.0
C(31)-P(2)-C(37)	109.3(2)	C(15)-C(14)-H(14)	120.0
C(25)-P(2)-C(37)	108.6(2)	C(16)-C(15)-C(14)	120.2(6)
C(43)-P(2)-C(37)	111.7(2)	C(16)-C(15)-H(15)	119.9
C(50)-C(49)-H(49A)	109.5	C(14)-C(15)-H(15)	119.9
C(50)-C(49)-H(49B)	109.5	C(15)-C(16)-C(17)	120.8(6)
H(49A)-C(49)-H(49B)	109.5	C(15)-C(16)-H(16)	119.6
C(50)-C(49)-H(49C)	109.5	C(17)-C(16)-H(16)	119.6
H(49A)-C(49)-H(49C)	109.5	C(16)-C(17)-C(18)	119.4(6)
H(49B)-C(49)-H(49C)	109.5	C(16)-C(17)-H(17)	120.3
C(50)-N(1)-C(51)	111.4(16)	C(18)-C(17)-H(17)	120.3
C(50)-N(1)-C(52)	128(2)	C(17)-C(18)-C(13)	121.0(5)
C(51)-N(1)-C(52)	120.3(18)	C(17)-C(18)-H(18)	119.5
C(2)-C(1)-C(6)	119.3(5)	C(13)-C(18)-H(18)	119.5
C(2)-C(1)-P(1)	123.3(4)	C(20)-C(19)-C(24)	119.4(5)
C(6)-C(1)-P(1)	116.8(4)	C(20)-C(19)-P(1)	120.0(4)
C(3)-C(2)-C(1)	120.2(5)	C(24)-C(19)-P(1)	120.5(4)
C(3)-C(2)-H(2)	119.9	C(19)-C(20)-C(21)	120.2(6)
C(1)-C(2)-H(2)	119.9	C(19)-C(20)-H(20)	119.9
C(2)-C(3)-C(4)	120.2(5)		

Table 5. (Continuation) Bond lengths [Å] and angles [°] for [1]

C(21)-C(20)-H(20)	119.9	C(38)-C(37)-P(2)	121.1(4)
C(22)-C(21)-C(20)	119.3(6)	C(42)-C(37)-P(2)	119.6(3)
C(22)-C(21)-H(21)	120.4	C(37)-C(38)-C(39)	120.4(5)
C(20)-C(21)-H(21)	120.4	C(37)-C(38)-H(38)	119.8
C(23)-C(22)-C(21)	121.3(6)	C(39)-C(38)-H(38)	119.8
C(23)-C(22)-H(22)	119.3	C(40)-C(39)-C(38)	119.9(5)
C(21)-C(22)-H(22)	119.3	C(40)-C(39)-H(39)	120.1
C(22)-C(23)-C(24)	120.0(6)	C(38)-C(39)-H(39)	120.1
C(22)-C(23)-H(23)	120.0	C(39)-C(40)-C(41)	120.7(5)
C(24)-C(23)-H(23)	120.0	C(39)-C(40)-H(40)	119.6
C(23)-C(24)-C(19)	119.6(6)	C(41)-C(40)-H(40)	119.6
C(23)-C(24)-H(24)	120.2	C(40)-C(41)-C(42)	119.8(5)
C(19)-C(24)-H(24)	120.2	C(40)-C(41)-H(41)	120.1
C(30)-C(25)-C(26)	119.6(4)	C(42)-C(41)-H(41)	120.1
C(30)-C(25)-P(2)	120.8(4)	C(41)-C(42)-C(37)	119.9(5)
C(26)-C(25)-P(2)	119.3(4)	C(41)-C(42)-H(42)	120.0
C(27)-C(26)-C(25)	119.7(5)	C(37)-C(42)-H(42)	120.0
C(27)-C(26)-H(26)	120.1	C(44)-C(43)-C(48)	118.8(4)
C(25)-C(26)-H(26)	120.1	C(44)-C(43)-P(2)	123.6(4)
C(28)-C(27)-C(26)	120.0(5)	C(48)-C(43)-P(2)	117.6(3)
C(28)-C(27)-H(27)	120.0	C(43)-C(44)-C(45)	120.2(5)
C(26)-C(27)-H(27)	120.0	C(43)-C(44)-H(44)	119.9
C(27)-C(28)-C(29)	121.0(5)	C(45)-C(44)-H(44)	119.9
C(27)-C(28)-H(28)	119.5	C(46)-C(45)-C(44)	120.1(5)
C(29)-C(28)-H(28)	119.5	C(46)-C(45)-H(45)	120.0
C(28)-C(29)-C(30)	119.5(5)	C(44)-C(45)-H(45)	120.0
C(28)-C(29)-H(29)	120.3	C(47)-C(46)-C(45)	120.0(5)
C(30)-C(29)-H(29)	120.3	C(47)-C(46)-H(46)	120.0
C(25)-C(30)-C(29)	120.2(5)	C(45)-C(46)-H(46)	120.0
C(25)-C(30)-H(30)	119.9	C(46)-C(47)-C(48)	120.6(5)
C(29)-C(30)-H(30)	119.9	C(46)-C(47)-H(47)	119.7
C(36)-C(31)-C(32)	119.0(4)	C(48)-C(47)-H(47)	119.7
C(36)-C(31)-P(2)	120.8(3)	C(47)-C(48)-C(43)	120.3(5)
C(32)-C(31)-P(2)	120.2(3)	C(47)-C(48)-H(48)	119.9
C(33)-C(32)-C(31)	119.7(4)	C(43)-C(48)-H(48)	119.9
C(33)-C(32)-H(32)	120.1	N(1)-C(50)-O(1)	127(2)
C(31)-C(32)-H(32)	120.1	N(1)-C(50)-C(49)	111.4(16)
C(34)-C(33)-C(32)	121.0(5)	O(1)-C(50)-C(49)	121.6(17)
C(34)-C(33)-H(33)	119.5	N(1)-C(51)-H(51A)	109.5
C(32)-C(33)-H(33)	119.5	N(1)-C(51)-H(51B)	109.5
C(33)-C(34)-C(35)	120.2(5)	H(51A)-C(51)-H(51B)	109.5
C(33)-C(34)-H(34)	119.9	N(1)-C(51)-H(51C)	109.5
C(35)-C(34)-H(34)	119.9	H(51A)-C(51)-H(51C)	109.5
C(34)-C(35)-C(36)	119.7(5)	H(51B)-C(51)-H(51C)	109.5
C(34)-C(35)-H(35)	120.1	N(1)-C(52)-H(52A)	109.5
C(36)-C(35)-H(35)	120.1	N(1)-C(52)-H(52B)	109.5
C(35)-C(36)-C(31)	120.3(4)	H(52A)-C(52)-H(52B)	109.5
C(35)-C(36)-H(36)	119.8	N(1)-C(52)-H(52C)	109.5
C(31)-C(36)-H(36)	119.8	H(52A)-C(52)-H(52C)	109.5
C(38)-C(37)-C(42)	119.3(5)	H(52B)-C(52)-H(52C)	109.5

Table 6. Atomic coordinates ($\times 10^4$) and equivalent isotropic displacement parameters ($\text{Å}^2 \times 10^3$) for $\text{P}2_1/c$.
 U(eq) is defined as one third of the trace of the orthogonalized U_{ij} tensor.

	x	y	z	U(eq)
W(1)	7995(1)	1211(1)	1452(1)	34(1)
Se(1)	9919(1)	1234(1)	1996(1)	54(1)
Se(2)	7398(1)	478(1)	1390(1)	45(1)
Se(3)	7289(1)	1615(1)	2572(1)	66(1)
Se(4)	7374(1)	1521(1)	-176(1)	45(1)
P(1)	997(1)	1245(1)	8319(1)	38(1)
P(2)	6109(1)	4071(1)	551(1)	33(1)
C(49)	4410(13)	2401(6)	6349(11)	215(8)
N(1)	3976(12)	2443(3)	7807(15)	223(8)
C(1)	132(4)	781(2)	8396(4)	38(1)
C(2)	-580(4)	778(2)	9006(4)	45(1)
C(3)	-1102(4)	390(2)	9144(4)	53(1)
C(4)	-907(4)	0(2)	8677(4)	53(1)
C(5)	-209(4)	2(2)	8058(4)	53(1)
C(6)	311(4)	389(2)	7915(4)	47(1)
C(7)	2347(4)	1148(2)	9186(3)	38(1)
C(8)	2668(4)	727(2)	9577(4)	45(1)
C(9)	3723(5)	659(2)	10208(4)	57(1)
C(10)	4464(5)	1000(2)	10453(5)	67(2)
C(11)	4153(5)	1416(2)	10070(5)	77(2)
C(12)	3094(4)	1494(2)	9434(5)	60(2)
C(13)	1071(4)	1275(2)	7012(4)	42(1)
C(14)	2074(5)	1311(2)	6788(4)	60(2)
C(15)	2098(6)	1341(2)	5766(5)	79(2)
C(16)	1136(6)	1335(2)	4980(5)	72(2)
C(17)	136(6)	1293(2)	5186(5)	66(2)
C(18)	106(5)	1264(2)	6198(4)	57(1)
C(19)	505(4)	1766(2)	8659(4)	44(1)
C(20)	310(5)	1817(2)	9611(5)	57(1)
C(21)	-66(5)	2218(2)	9877(6)	72(2)
C(22)	-202(5)	2571(2)	9200(7)	81(2)
C(23)	25(5)	2532(2)	8281(6)	78(2)
C(24)	368(5)	2127(2)	7989(5)	59(2)
C(25)	4979(4)	4012(2)	-608(3)	36(1)
C(26)	4291(4)	3645(2)	-721(4)	51(1)
C(27)	3362(4)	3617(2)	-1565(4)	61(2)
C(28)	3134(5)	3947(2)	-2289(4)	63(2)
C(29)	3807(5)	4310(2)	-2192(4)	58(1)
C(30)	4733(4)	4344(2)	-1342(4)	46(1)
C(31)	5586(3)	4283(1)	1566(3)	34(1)
C(32)	4487(4)	4419(2)	1347(4)	41(1)
C(33)	4102(4)	4591(2)	2125(4)	49(1)
C(34)	4773(4)	4620(2)	3119(4)	49(1)
C(35)	5854(5)	4482(2)	3353(4)	51(1)
C(36)	6269(4)	4322(2)	2574(4)	44(1)
C(37)	7090(4)	4460(1)	301(3)	35(1)

Table 6. (continuation) Atomic coordinates ($\times 10^4$) and equivalent isotropic displacement parameters ($\text{Å}^2 \times 10^3$) for $\text{P}2_1/c$.
 U(eq) is defined as one third of the trace of the orthogonalized U_{ij} tensor.

C(38)	7341(4)	4849(2)	854(4)	47(1)
C(39)	8063(4)	5154(2)	624(4)	53(1)
C(40)	8545(4)	5063(2)	-142(4)	51(1)
C(41)	8308(4)	4676(2)	-705(4)	55(1)
C(42)	7576(4)	4373(2)	-490(4)	50(1)
C(43)	6713(4)	3530(2)	883(3)	37(1)
C(44)	6977(5)	3356(2)	1869(4)	57(1)
C(45)	7424(6)	2933(2)	2061(5)	72(2)
C(46)	7610(5)	2687(2)	1269(5)	63(2)
C(47)	7373(5)	2860(2)	301(5)	61(2)
C(48)	6924(4)	3279(2)	97(4)	52(1)
O(1)	2529(11)	2616(5)	6388(11)	326(8)
C(50)	3607(12)	2505(4)	6904(13)	177(8)
C(51)	3198(8)	2484(3)	8303(10)	129(5)
C(52)	5055(10)	2314(5)	8351(11)	206(7)
